ARTICLE

Check for updates

A framework to assess multi-hazard physical climate risk for power generation projects from publicly-accessible sources

Tianyi Luo [1✉], Yan Cheng [2], James Falzon [3], Julian Kölbel [4], Lihuan Zhou[5], Yili Wu[6] & Amir Habchi[3]

Demand for information about physical climate risk is growing, particularly for the power generation sector, given its size and pronounced exposure to climate hazards. However, quantifying physical climate risks for a large number of assets remains challenging. Here we introduce a scalable and transparent methodology that enables multi-hazard physical climate risk assessments for any thermal or hydro power generation project. The methodology relies on basic power plant type and geolocation data inputs, publicly-available climate datasets, and hazard- and technology-specific vulnerability factors, to translate hazard severity into generation losses. We apply the methodology to the European Bank for Reconstruction and Development's early 2021 thermal and hydro power generation portfolios of 80 assets. We show that under the Representative Concentration Pathway 4.5 scenario, those 80 power plants could experience a 4.0-10.9 TWh loss in annual generation (or 1.87-5.07% of total annual maximum generation) by 2030 compared to its baseline losses of 0.70–0.87 TWh (or 0.33–0.41%). One of the largest drivers of the increased risk is rising water temperatures, which is currently overlooked by mainstream climate risk disclosure guidelines.

[1] Bluerisk, Beijing, China. [2] University of Copenhagen, Copenhagen, Denmark. [3] The European Bank for Reconstruction and Development, London, UK. [4] University of St. Gallen, St. Gallen, Switzerland. [5] The World Resources Institute, Washington DC, USA. [6] Global X ETFs, New York, NY, USA. ✉email: tianyiluo@blueriskintel.com

Physical climate risk has become a major concern for governments, companies, and civil societies[1,2]. There are both proprietary (e.g., Moody's ESG360, BlackRock Aladdin, Swiss Re CatNet) and publicly available tools (e.g., the World Bank Climate Change Knowledge Portal, the World Resources Institute Aqueduct Water Risk Atlas) that aim to help their users understand and assess physical climate risks. However, many of those tools can only provide analyses and estimates on physical climate hazard exposure rather than physical climate risks, which is typically defined as a function of hazard, exposure, and vulnerability;[3] Some commercial tools do provide risk estimates, but with fixed vulnerability factors hidden behind proprietary methodologies[4]. As such, their results are useful for basic risk exposure screening, but are of limited usefulness when assessing impact.

Physical risks of climate change are especially relevant for the power sector. The power sector is strongly exposed to physical climate risks[5–8]. Several studies demonstrate the vulnerability of the power sector. Studies have investigated generation losses (one of the most relevant metrics required for financial modeling) due to water scarcity[9–14], extreme weather events[15,16], outages for nuclear power plants[17], as well as entire energy systems[18]. Yet these prior approaches mostly focus on a specific hazard and often require local input data (e.g., observed weather data, river gauge discharge records, actual power-generation records) that is hard to access or proprietary. Inconsistent or unavailable input data is a key impediment for comparing and integrating empirical assessments of physical risk[6]. Without quantifying physical climate risks in metrics such as generation losses, we cannot properly include climate impact in our decision-making.

We introduce a methodology to quantify multi-hazard physical climate risks in generation losses for any given thermal and hydropower plant, leveraging publicly-available global datasets.

Our model takes plant-specific type and geolocation data based on which relevant local climate and water time-series data are extracted from gridded global datasets, and assesses potential generation losses due to climate hazards for both present day and the future. We pilot-test the model on the European Bank for Reconstruction and Development's (EBRD) early 2021 thermal (including gas, coal, nuclear, oil, and geothermal) and hydro-power generation portfolios (excluding solar and wind). We contribute a versatile risk assessment model that is both generalizable and scalable. The data requirements on power plants are minimal, and the hazard modules and vulnerability factors are fully transparent, allowing for customization and further development.

Modeling approach. We follow the Intergovernmental Panel on Climate Change's climate risk function[19] which determines risks with exposure and vulnerability levels if specific hazards occur, and develop our methodology with the aim to allow for transparent power plant physical climate risk assessments using publicly available gridded global data on climate and water baselines and future projections with minimal data required on plants or locally sourced information. The only required power plant data inputs are its geolocation, generation technology, cooling type (if applicable), and installed capacity, all of which are basic information and usually available in power plant databases (e.g., Global Power Plant Database[20]).

Our model considers seven different hazards in five mutually exclusive modules as shown in Table 1 and Supplementary Fig. 1. The selection of hazards is based on existing mainstream climate disclosure guidelines[21,22], materiality, sectoral relevance, and data availability. The five modules include air temperature, water temperature, water stress, floods, and droughts for modeling.

Table 1 Physical climate risk assessment modules in the power sector.

| Modules	Physical climate hazards covered	Main impact mechanisms	Key thresholds
Water temperature	Sustained water temperature rise;[29,42,53] Extreme temperature (water)[29,42,53]	Water temperature primarily affects a power plant's cooling efficiency and/or its ability to meet local regulatory discharge temperature standards. It has no impact on gas turbines or air-cooled units.	Regulatory discharge temperature limits; design cooling water temperature; baseline p99 web-bulb air temperature
Air temperature	Sustained air temperature rise;[29,54] Extreme temperature (air)[29,54]	Air temperature primarily affects the generation efficiency of gas turbines and cooling efficiency of air-cooling systems. Additionally, wet-bulb air temperature (determined by the combined conditions of air temperature and relative humidity) affects cooling efficiency of recirculating cooling towers. Air temperature also affects water releases from glaciers impacting downstream water available to dams.	Design operating air temperature
Water stress	Water stress[55,56]	In high water-stress areas, decreased water availability - whether caused by reduced runoff or increased demand/competition - can result in reduction in permitted water withdrawals and/or more stringent water efficiency regulations in the future. Upstream water consumption affects downstream water available to dams.	Regulatory water use limits
Floods	Riverine and coastal floods;[33] Sea-level change[33]	When flood water inundated a power plant, operations are disrupted due to infrastructure damage and/or mechanical failure.	Depth-damage function
Droughts	Droughts (temperature effects excluded)[29,54,57]	Water levels in rivers and/or reservoirs are low during droughts; wet-cooled plants might lose access to cooling water or not have sufficient flow rates for cooling effect. Low river flow can also affect hydro generation.	SPEI-disruption function
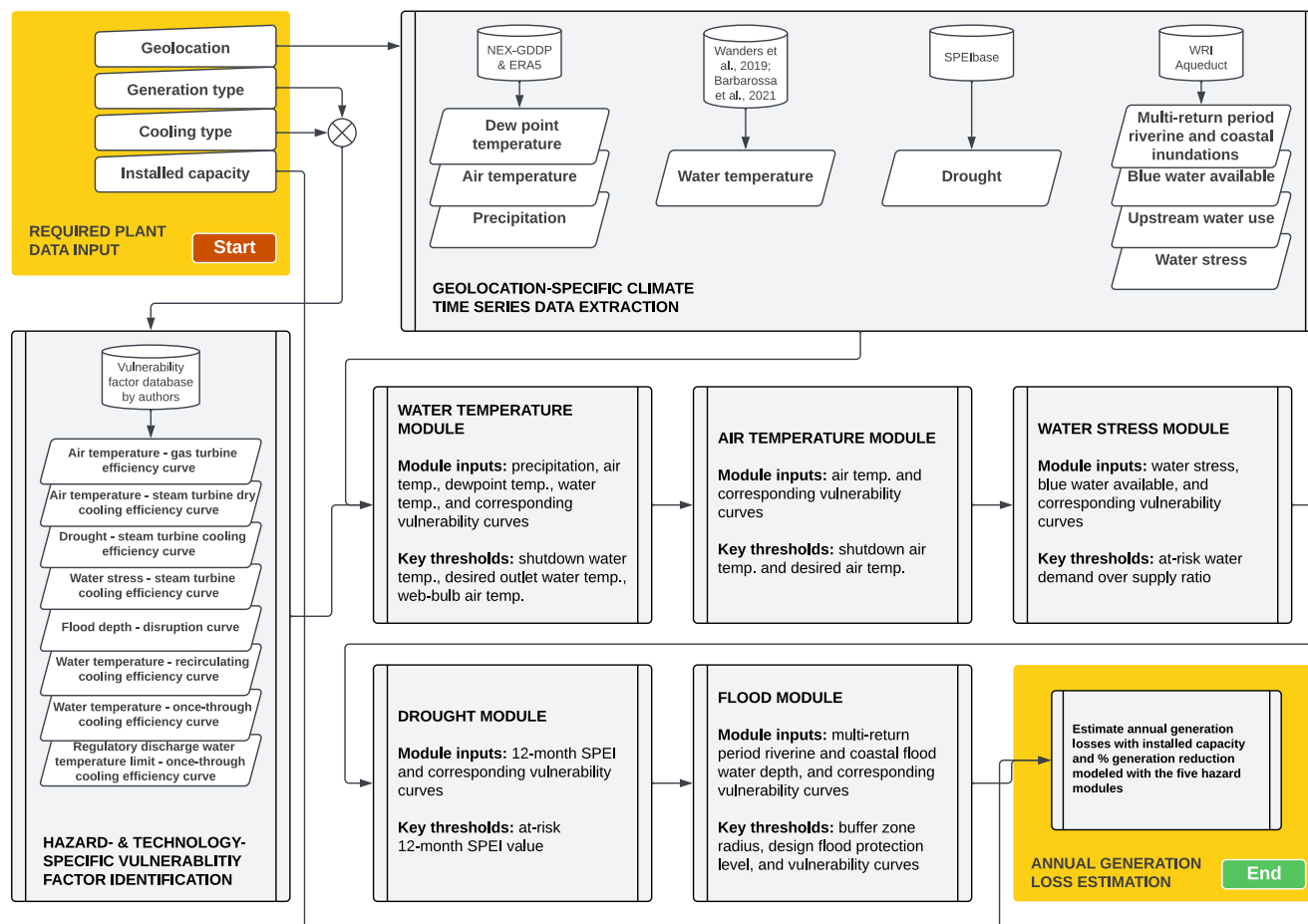
Fig. 1 Schematic representation of the power generation sector-specific physical climate risk assessment model. Details on threshold setting, vulnerability factors, and modules can be found in "Methods".

Due to the inconsistencies between the climate forcings (see the Limitations section for more detail) of current climate and water datasets, the spatial and temporal correlations between hazards are not explicitly studied.

Exposure is based on the plant's geolocation (e.g., latitude and longitude), generation technology, and cooling type (when applicable). Plant geolocation data are used to extract baseline and projected climate and water data from global gridded datasets with spatial resolution ranging from 1 to 25 km. Generation technology and cooling-type data are used for selecting the correct vulnerability factors for each hazard.

Vulnerability factors (or damage functions/curves) for translating hazard severity into generation losses are collected from the literature or developed based on expert consultation. Vulnerability factors are specific to the hazard and the power production technology, i.e., combinations of generation technology (e.g., gas turbines) and cooling type (e.g., natural draft tower wet cooling). Detailed factors are provided in Supplementary Table 1.

The baseline period used in our model runs from 1965 through 2004, and the future 2030 period is from 2010 through 2049, a 40-year window centered around 2030. The end year of the baseline period is determined due to the fact that in the Coupled Model Intercomparison Project Phase 5 (CMIP5), the historical scenario ends in 2005, and rcp45 and rcp85 projection scenarios start in 2006. Climate backcast data in the historical scenario are used to bias-correct the reanalysis data in the baseline period as needed. We conduct assessments under two climate scenarios, Representative Concentration Pathway (RCP) 4.5 and 8.5, representing potential climate impact from moderate to the most extreme.

The climate models used in our assessment are from CMIP5. We use an ensemble approach for all risk modules. In this study, unless otherwise stated, all generation loss estimates are reported as ranges using the p10 and p90 values of the ensemble. These thresholds are commonly used in risk analysis, but for robustness we perform a sensitivity analysis in the "Methods".

As illustrated in Fig. 1, our modeling process starts by taking four data points as inputs for a given power plant when assessing its physical climate risks. First, based on the plant's latitude and longitude, our model pinpoints the location in the gridded global climate and water datasets, and extracts and processes the baseline and future projection time series data for each climate hazard and for each climate scenario and each Global Climate Model (GCM). Second, based on the generation technology and cooling type (when applicable) combination, our model identifies for each hazard the vulnerability curves for that particular generation-cooling combination from the vulnerability factors database the authors developed. Third, the model runs the hazard time series data and corresponding vulnerability curves through each of five modules, and generates for each of seven hazards its annual average generation loss percentage. Finally, annual average generation losses are estimated based on the plant's installed capacity and hazard-specific loss percentages. Detailed step-by-step descriptions on model and methodologies can be found in "Methods".

EBRD's portfolio and its exposure to climate change. EBRD's current (a snapshot from early 2021) thermal portfolio consists of
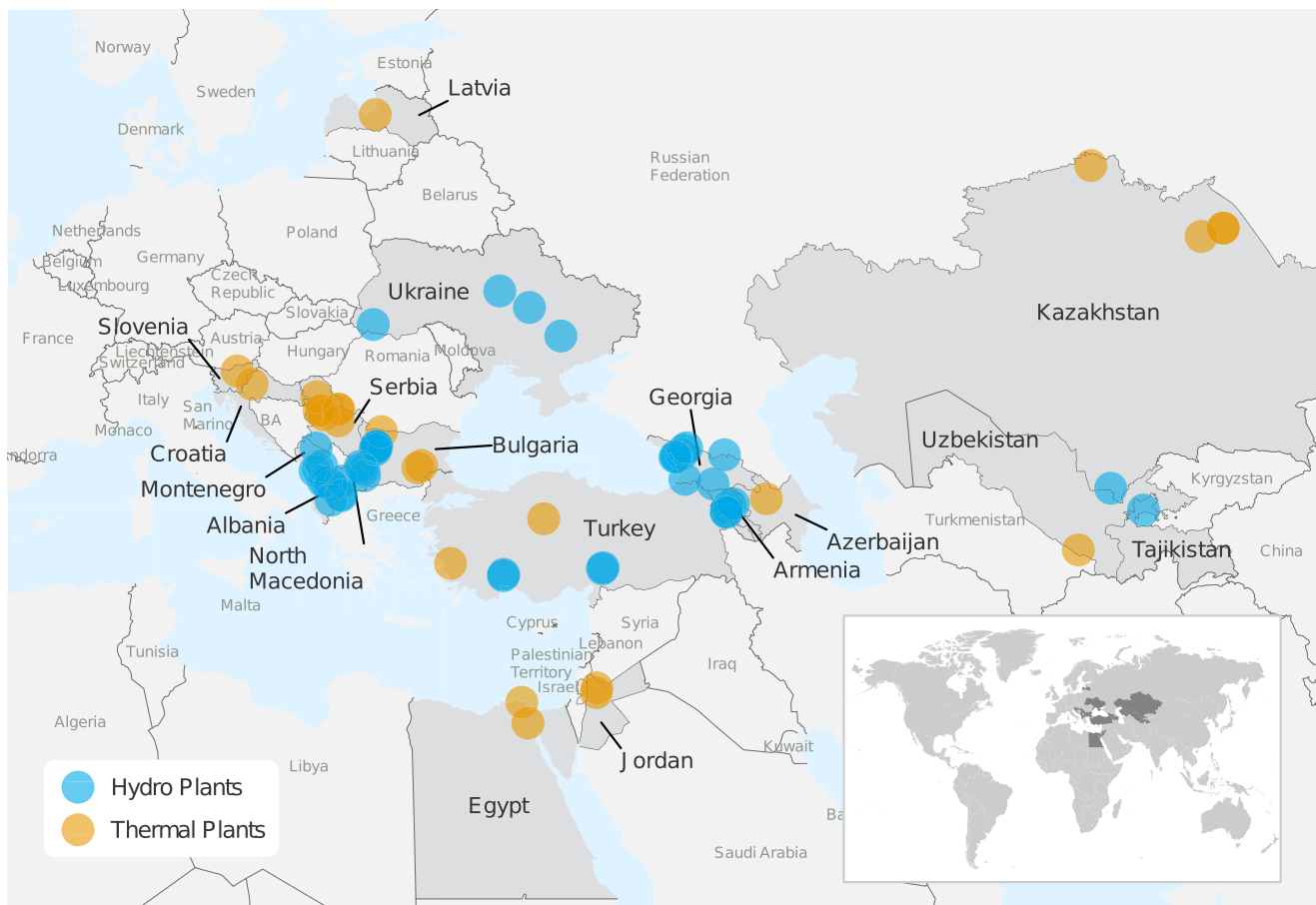
Fig. 2 Spatial distribution of power plants in EBRD's current thermal and hydropower-generation portfolios. The thermal power plants are denoted with orange circles while the hydropower plants are denoted with blue circles.

80 power plants (24 thermal and 56 hydropower) with a variety of fuel types including natural gas, coal, nuclear, oil, and geothermal, spanning across Eastern Europe, southern Mediterranean, and Central Asia. Thermal power plant generation units range from an installed capacity of 25 MW to 1000 MW using different types of cooling systems, and account for over 74% of the total installed capacity (22.6 GW) of the thermal and hydro portfolios. The EBRD portfolio exhibits a higher number of smaller generation units, and 87% of units have an installed capacity below 300 MW. Cooling systems used in thermal power plants include once-through, recirculating, and air-cooling. Over half of the thermal capacity in EBRD's portfolio uses once-through cooling systems. Recirculating and dry cooling systems each represent about a quarter of EBRD's thermal portfolio. In EBRD's current hydro portfolio, most hydro plants are small or mini hydro projects.

The regions EBRD operates in are among the most vulnerable to climate change. Figure 2 illustrates the locations of all 80 power plants in EBRD's current thermal and hydropower generation portfolio. Figure 3a, b shows that a typical (the median value of the climate model ensemble) power plant in EBRD's portfolio is likely to see a monthly average air temperature increase by 11.3% and precipitation increase by 2.3% between the baseline and 2030 under RCP4.5, and 12.7% and 3.2% under RCP8.5. In addition, extreme weather events are expected to become more intense in all areas of EBRD's portfolio. Figure 3c, d illustrates that for a typical power plant, the 12-month low precipitation is expected to decrease by 5%, and the maximum air temperature is expected to increase by 8.5% by 2030 under RCP4.5, and 8% and 9.7% under RCP8.5. As a result of global warming, the majority of EBRD's

power plants equipped with wet-cooling technologies are projected to experience a substantial water temperature rise at their cooling water intake points. Figure 3e suggests that the water temperature could increase by 10.7–13.5% (1.4–1.9 °C) by 2030 under RCP4.5 and RCP8.5, respectively.

Results

We estimate that, for EBRD's current thermal and hydropower generation sector portfolio, its physical climate risk-driven annual average generation losses are about 0.70–0.87 TWh (or 0.33–0.41% of total maximum annual generation) for the baseline period. As shown in Fig. 4 and Table 2, that could grow to 4.0–10.9 TWh (1.87–5.07%) by 2030 under RCP4.5, and to 4.5–11.4 TWh (2.08–5.32%) under RCP8.5. The thermal power plants in EBRD's portfolio account for 97–98% of the increase in physical climate risk-driven generation losses, while the rest is driven by hydro plants. A previous study[23] also suggests a reduced usable capacity of thermal and hydropower plants globally under the same climate scenarios, and concludes that hydro plants are generally less vulnerable to future climate change than thermal plants at the global scale. Figure 4 and Table 2 illustrate the breakdown of potential generation losses by driver, by time period, and by scenario. Uncertainties of climate models are also presented, with the 90th percentile (p90) of the ensemble being the upper bound and 10th percentile (p10) the lower bound.

Water temperature is one of the primary drivers of generation losses, accounting for 0.6 TWh for the baseline, and 1.9–4.6 TWh by 2030 under RCP4.5, and 2.3–5.3 TWh under RCP8.5. For the
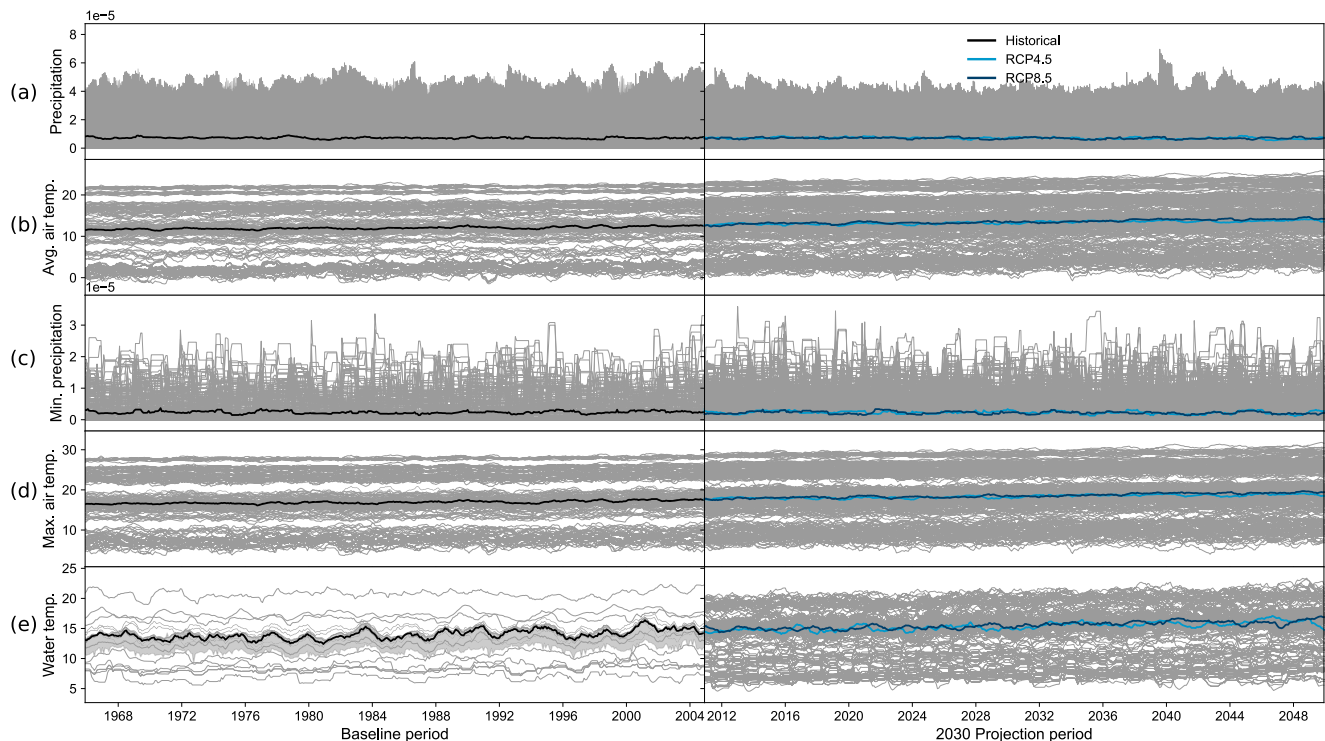
Fig. 3 Precipitation, air temperature, and water temperature trends from baseline to the 2030 projection period. a shows precipitation, **b** average air temperature, **c** minimum precipitation, **d** maximum air temperature, and **e** water temperature. Gray lines represent simulations by a climate model, by scenario, and by power plant. Black and blue lines are the ensemble medians of historical values and projections under RCP4.5 and RCP8.5.
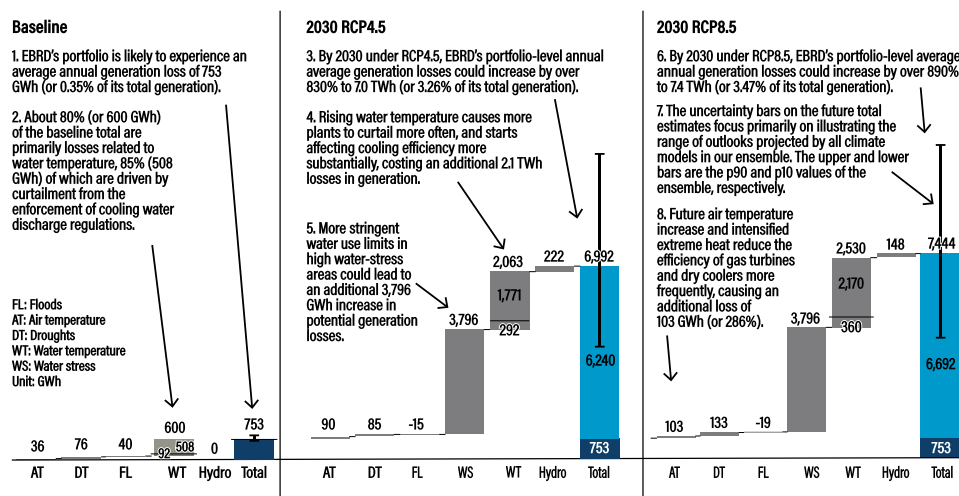

Fig. 4 EBRD's estimated portfolio-level physical climate risk-induced generation losses for the baseline period and by 2030 under RCP4.5 and RCP8.5. Generation loss estimates reported in the text in the figure are ensemble medians. The vertical line on each total bar indicates the climate model-induced uncertainties, i.e., the lower bound is the 10th percentile (p10), and the upper bound is the 90th percentile (p90). For thermal plants, the physical climate risks are categorized according to the climatic variables, i.e., air temperature (AT), droughts (DT), floods (FL), water stress (WS), and water temperature (WT). Water temperature bars are divided into two parts with a black horizontal line. The lower part represents the cooling efficiency reduction-caused generation losses, and the upper is generation losses driven by curtailment from cooling water discharge regulation enforcement. There are 80 power plants.

baseline, about 85% of the total water temperature-driven generation losses is driven by reduced production required for compliance with cooling water discharge regulations, and the rest by reduced cooling efficiency. Cooling water discharge temperature regulations affect only power plants with once-through cooling systems. Recirculating cooling systems are typically designed to operate with optimal performance when the wet-bulb temperature is below the p99 value of its historical records[24].

With temperatures rising at most EBRD power plants' cooling water intakes, once-through systems could expect more frequent shutdowns if discharge regulations are enforced, and the performance of recirculating towers and condensers is set to reduce as the baseline p99 values have a much higher probability of occurring in the future. Water stress is also a major driver that could potentially cause EBRD's portfolio an annual average generation loss of 2.0–3.8 TWh by 2030 under RCP4.5 and

Table 2 EBRD's estimated portfolio-level physical climate risk-induced generation losses (MWh) for the baseline period and by 2030 under RCP4.5 and RCP8.5.

Driver	Baseline			2030 RCP4.5			2030 RCP8.5		
	median	p10	p90	median	p10	p90	median	p10	p90
Thermal	752,761 (0.35%)	699,082 (0.33%)	872,503 (0.41%)	6,770,519 (3.15%)	4,012,516 (1.87%)	9,219,146 (4.29%)	7,296,154 (3.40%)	4,474,983 (2.08%)	9,920,404 (4.62%)
Air temperature	36,497 (0.02%)	33,180 (0.02%)	42,838 (0.02%)	126,033 (0.06%)	93,186 (0.04%)	170,772 (0.08%)	139,485 (0.06%)	116,168 (0.05%)	192,341 (0.09%)
Droughts	76,420 (0.04%)	26,058 (0.01%)	189,821 (0.09%)	161,058 (0.08%)	47,009 (0.02%)	523,126 (0.24%)	209,755 (0.10%)	44,960 (0.02%)	589,018 (0.27%)
Floods	39,531 (0.02%)	NA	NA	24,634 (0.01%)	9373 (0.004%)	91,586 (0.04%)	20,680 (0.01%)	18,577 (0.01%)	51,174 (0.02%)
Water stress	NA	NA	NA	3,795,781 (1.77%)	1,955,081 (0.91%)	3,795,781 (1.77%)	3,795,781 (1.77%)	1,955,081 (0.91%)	3,795,781 (1.77%)
Water temperature	600,313 (0.28%)	NA	NA	2,663,012 (1.24%)	1,907,868 (0.89%)	4,637,881 (2.16%)	3,130,452 (1.46%)	2,340,198 (1.09%)	5,292,090 (2.46%)
Efficiency reduction	92,236 (0.04%)	NA	NA	383,915 (0.18%)	267,406 (0.12%)	730,217 (0.34%)	452,377 (0.21%)	335,596 (0.16%)	794,060 (0.37%)
Discharge water limits	508,077 (0.24%)	NA	NA	2,279,097 (1.06%)	1,640,461 (0.76%)	3,907,664 (1.82%)	2,678,074 (1.25%)	2,004,602 (0.93%)	4,498,029 (2.10%)
Hydro	NA	NA	NA	221,774 (0.10%)	−6,854 (0.003%)	1,673,598 (0.78%)	148,253 (0.07%)	−4,090 (0.002%)	1,494,616 (0.70%)
Total	752,761 (0.35%)	699,082 (0.33%)	872,503 (0.41%)	6,992,293 (3.26%)	4,005,663 (1.87%)	10,892,745 (5.07%)	7,444,407 (3.47%)	4,470,894 (2.08%)	11,415,020 (5.32%)

The 10th percentile (p10) and 90th percentile (p90) values of the ensemble are calculated to quantify uncertainties introduced by climate models. NA, or Not Applicable, refers to cases where model-specific estimates are not available when data are forced with climate reanalysis instead of backcasts. Percentages in brackets are the % generation losses over the total annual generation of the entire portfolio.

RCP8.5, if more stringent water use limits were introduced due to increased stress levels and no mitigation efforts made at the plant level. Water stress levels increase because of either the growing local water demand or reduction of water supplies, or both, which is the case for many plants in EBRD's portfolio. High water stress levels very often lead to greater uncertainties in water regulations. Power plants with water-inefficient systems or practices are particularly vulnerable to higher environmental standards and strengthened regulations on water withdrawal and consumption limits. Air temperature increase could cause EBRD's current portfolio 0.03–0.04 TWh in generation losses on average every year for the baseline period, and 0.09–0.17 TWh by 2030 under RCP4.5 and 0.12–0.19 TWh under RCP8.5, since air temperature affects gas turbine and dry cooling system efficiencies. Generation losses associated with wet-bulb temperature for recirculating plants are accounted for in the water temperature assessment module. Drought is estimated to account for 0.03–0.19 TWh in generation losses for the baseline period, and 0.05–0.52 TWh by 2030 under RCP4.5, and 0.04–0.59 TWh under RCP8.5. In our drought assessments, we focus on generation losses caused by reduced cooling water accessibility. The impact of extreme water temperatures associated with drought events is accounted for in the water temperature assessment module.

As precipitation decreases and water consumption increases in most upstream watersheds of the hydro plants in EBRD's portfolio, we estimate a −7 to 1674 GWh change in annual average generation by 2030 under RCP4.5, and −4 to 1495 GWh under RCP8.5, at the portfolio level. Air temperature rises also negatively affect water availability in most cases, as higher temperature typically leads to more evaporation thus reduced water supply. However, for hydro plants located in watersheds where glaciers exist, rising air temperature could contribute to more glacier melt which leads to more water supply and potentially additional generation in the short term. For most hydro plants in EBRD's portfolio, we use plant-specific upstream precipitation and water consumption changes between now and 2030 to estimate their potential generation changes due to water availability shifts. Air temperature is not included because the climate and water datasets we use do not account for glacier impact. For six hydro plants, actual historical generation and operations data were made available by EBRD to the authors, and deep-dive analyses were conducted leveraging a machine learning-based regression model. Detailed descriptions of the methodology can be found in "Methods".

Certain power plant specifications can be custom designed to adjust for local climate conditions to achieve better performance in places with less-than-desirable conditions. However, those customizations are designed using historical climate records, and are anticipated to experience increases in their exceedance probabilities. In this study, we use the p90 value of the baseline daily average air temperature of each power plant location as that plant's design air temperature. The same assumptions are made for cooling water intake temperatures. As illustrated in Fig. 5a, for air-cooled plants in EBRD's portfolio, sustained air temperature rise projected under RCP4.5 could increase the exceedance probability of their design air temperature from 10% to 18–25%. Sustained water temperature rise will lead to an increase in design water temperature exceedance probability for most of the wet-cooled plants in the portfolio, from 10% to up to 27%, as shown in Fig. 5b.

As shown in Fig. 6a and Table 3, a typical CCGT plant in EBRD's portfolio has roughly the same percentage loss in generation as that of a typical coal-fired power plant for the baseline period. However, by 2030, coal-fired power plants are projected to see the percentage loss increase to 1.7% under RCP4.5 and 2.1% under RCP8.5, more than twice as high as that of CCGT plants. In other words, we believe that the CCGT plants in EBRD's portfolio are substantially more climate-resilient than the
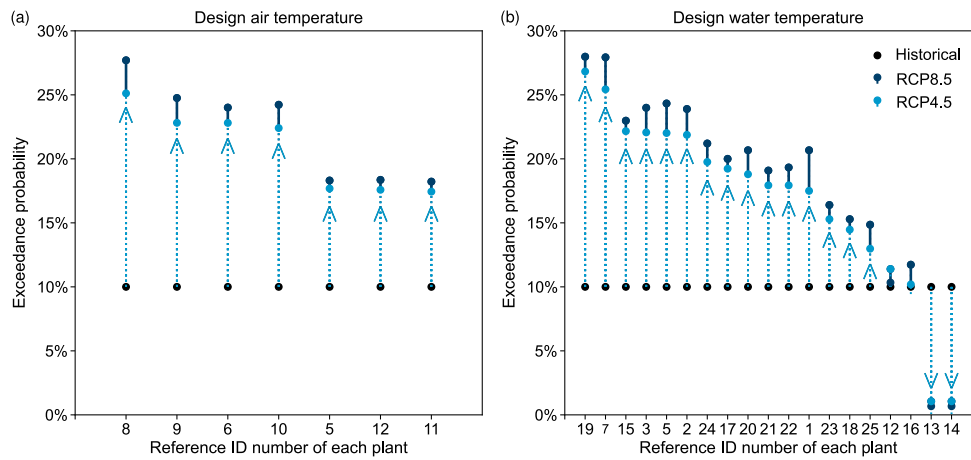
Fig. 5 Exceedance probability of design air and water temperatures in baseline and future periods by power plants. a represents designed air temperatures. **b** represents designed water temperatures. The direction of the arrow at the end of each vertical line indicates the changing trend for each plant. The vertical lines in both plots are sorted in descending order of the probability under RCP4.5.
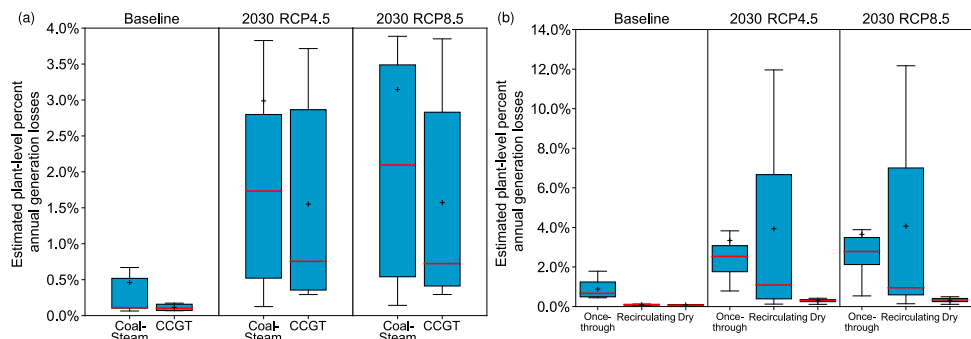

Fig. 6 Plant-level physical climate risk-induced generation losses. a shows the generation losses grouped by generation type; **b** by cooling technology. The red line inside each box is the median. The black crosses are the mean values. The box shows the 25th (Q1) and 75th (Q3) percentile, and the upper whisker extend to Q3 + 1.5 * (Q3–Q1) and the lower to Q1–1.5 * (Q3–Q1). The plant counts are in Table 3.

Table 3 Ensemble statistics of plant-level physical climate risk-induced generation losses by generation type and by cooling technology.

Plant type	Plant count	Baseline			2030 RCP4.5			2030 RCP8.5		
		Median	**p5**	**p95**	**Median**	**p5**	**p95**	**Median**	**p5**	**p95**
Fuel-Turbine										
Coal-Steam	13	0.11%	0.07%	1.60%	1.73%	0.13%	11.76%	2.10%	0.14%	11.93%
CCGT	6	0.10%	0.07%	0.17%	0.76%	0.30%	3.65%	0.72%	0.32%	3.75%
Cooling										
Once-through	9	0.67%	0.45%	1.66%	2.53%	1.17%	8.16%	2.78%	1.16%	8.83%
Recirculating	11	0.10%	0.05%	0.15%	1.09%	0.13%	11.79%	0.95%	0.14%	11.97%
Dry	4	0.07%	0.04%	0.16%	0.31%	0.14%	0.41%	0.34%	0.14%	0.48%

coal-fired power plants. Previous study[25] also found that CCGT plants are expected to experience smaller annual generation reductions than coal-fired plants in the United States. In terms of cooling technology, as shown in Fig. 6b, a typical once-through cooled power plant has a much higher percentage loss compared to plants cooled with recirculating or dry systems, for both the baseline and future periods, which agrees with the previous research[26]. However, our analysis shows that advanced cooling systems are also subject to increased physical climate risks. Percentage losses in the generation of plants equipped with recirculating systems jump from 0.1% to about 1% under both climate scenarios. Dry-cooled plants are projected to see a slight increase

in percentage losses; however, it remains very low in absolute terms at roughly 0.3%.

Validation at the portfolio and plant level

Plant-level actual generation data are typically considered strictly confidential, particularly in countries where EBRD invests, and the authors were not able to obtain that information for any of the thermal plants or most of the hydro plants in EBRD's portfolio. Given the lack of generation data available for the thermal power plants in EBRD's portfolio, we aim to validate our thermal assessment models in the following two ways. One is to compare

our baseline portfolio-level, percentage losses with another portfolio (with a similar power mix) for which we have actual disruption data which can be used in calculating actual physical climate hazard-induced generation losses. The other is to apply our modules over power plants which we have actual daily generation data for, and compare model-estimated generation losses against actual losses induced by climate. For validating with the two proposed approaches, we use unit-level daily outage data for thermal power plants in India from April 1, 2013 through March 31, 2017 as well as unit-level daily generation data from January 1, 2013 through December 31, 2016 of two Indian CCGT power plants from a previous study[27]. The outage database has daily records of all generating units that are shut down on each day, including their installed capacity and the reason why they were taken offline.

For portfolio-level validation, we analyze the outage database, and categorize outage reasons into two groups, physical climate hazard-related and others. For units with physical climate hazard-related outages, we calculate for each unit on each day how much power it could have generated if it were working at full capacity. Those generation losses are then compared with the maximum annual generation of India's entire thermal (including nuclear) and hydropower fleet[28], resulting in a percentage annual generation losses ranging from 0.239 to 0.801% between the fiscal year 2014 and 2017, with the average being 0.496% and standard deviation 0.238%. As shown in Supplementary Fig. 2a, our baseline ensemble of generation losses estimated for EBRD's current portfolio has a median of 0.351%, and a p5 value of 0.326% and a p95 of 0.406%, which fall in the same ballpark as the Indian portfolio estimates.

For plant-level validation, we assess the impact of high air temperature on generation using daily generation data of the Uran and Valuthur CCGT power plants. The two plants are selected as they are the only CCGT plants that have generation records for a few years overlapped with the period for which we have climate data. The few other CCGT plants the Government of India publishes data for have either very recent generation histories or very patchy records of production, which made them unfit for plant-level validation. Plant selection for validation in this study has limitations, including the uncertainties in gas plant operation schemes as well as the differences in local climate and temperatures between Western and Southern India and EBRD regions. The air temperature reanalysis for each power plant is extracted from the ERA5 database[29]. As illustrated in Supplementary Fig. 3, both Uran and Valuthur have two distinct operation schemes. We classified two clusters using DBSCAN[30] and applied an Ordinary Least Squares (OLS) linear regressions to each cluster to model the correlation between power generation and air temperature. As Supplementary Fig. 2b shows, using the fitted regressions, between 2013 and 2016, we estimate that high air temperature-induced percentage generation losses for Uran and Valuthur has an average of 0.031% and a standard deviation of 0.019%. Using the air temperature module in our proposed model, the average percentage generation loss is 0.055% with a standard deviation of 0.004%, which has the same order of magnitude as the regression-based results. Details on the calculations can be found in the Methods.

Discussion

There are several factors contributing to the potential wide applicability of the methodology proposed by this study. First, only four basic input data points are required by the model for assessing any given power plant's physical climate risks. Second, with the latitude and longitude of a given power plant, location-specific baseline and future projections of the climate- and water-related hazard time series data required by the different modules in the methodology can be extracted from publicly-available, global climate and water datasets identified by the authors. By leveraging global gridded datasets, the methodology addresses typical climate data challenges such as global coverage and comparability. Third, translating hazard severity to decision-relevant risk metrics such as generation losses can be achieved by leveraging the global average hazard- and technology-specific vulnerability factors (or damage functions) database developed by the authors from extensive literature review and expert consultation. The vulnerability factor database enables users to conduct assessments when local vulnerability information is not available which is typically a reality faced by financial institutions with a large portfolio and a global footprint. Finally, the transparent, modular approach also allows for model customization, e.g., updating vulnerability factors and hazard data and customizing key thresholds, so that users could get more robust results if more accurate, locally calibrated or observed data are available.

The scalability of our methodology is promising in our opinion for three reasons. First, it takes about two hours for the model to complete for one asset the entire risk assessment process from climate data retrieval to hazard module processing, and it can assess multiple assets without any interference required from outside the model. Second, the average per-plant model runtime could be reduced when assessing portfolios with clusters of power plants located close by and in the same watersheds. The most time-consuming part of the exercise is climate data retrieving and processing. If multiple plants are located in the same pixel or watershed, climate data for that location can be retrieved and processed just once and used for all plants. Finally, the total runtime required for modeling a portfolio can be further reduced if fewer climate scenarios and GCMs are required or if that portfolio can be divided into smaller chunks which can be assessed in parallel.

The proposed methodology provides assessment results in power-generation losses which is a key data point needed by financial analysts for properly integrating physical climate risk in project valuation. For example, a development bank investment officer can adjust the loan structure of a power-generation project to better account for and protect the bank's investment from climate impacts, if the project's financial modeling shows that physical climate risk-induced generation losses would affect the project's ability to generate revenue or to pay back loans in the future. Further translating future plant generation losses to revenue losses or to the probability of default requires project-level financial models and information on the embedded assumptions which are typically asset specific and in most cases strictly confidential. The authors choose to focus on compiling publicly-available data sources and developing a methodology that estimates plant-level power-generation losses which in our opinion brings more value to the subject than attempting to assign a monetary value to risks without project-specific financial models to which the authors have no access.

Power plants are particularly vulnerable to water-related physical climate hazards. In addition to acute, extreme weather events such as heatwaves, droughts, and floods, we demonstrate chronic physical hazards, e.g., water temperature and water stress, can cause large impact on generation capabilities as climate changes. Most power plants today are designed on the basis of historical rather than future climate and our assessment shows that those chronic hazards are very likely to emerge in the coming decades and cause the largest disruptions. In particular, water temperature is completely overlooked right now by mainstream climate disclosure guidelines. Additionally, these hazards are usually not covered by insurance products, meaning exposed assets would not be able to transfer these risks. It is crucial that chronic physical climate risks are assessed and their impact quantified.

Fossil fuel-based thermal power plants and hydropower account for the majority of world's power generation as well as a large share of global carbon emissions. For the power sector as a whole to become more resilient to climate change, understanding how its largest share of power-generation sources could be affected by climate change is an important first step. The methodology developed and data compiled in this study could be useful to many power utility asset managers and development banks as the many assets in their portfolios are thermal and hydro plants. However, as solar and wind projects become increasingly large in their footprints, additional research that incorporates solar and wind projects could help understand the magnitude of physical climate risks to these technologies, providing a more complete assessment of the portfolio's physical risk.

Gaps in global climate and hydrology data still remain. Researchers and data developers should continue to improve the coverage, comparability, and granularity of climate hazard data, particularly on future runoff, water temperature, flooding, and wind, and make data available to the public. Open data coverage of more climate hazard types can help fill some of the current gaps and enhance the overall comprehensiveness of physical climate risk assessment. Making climate data more comparable and granular will reduce system uncertainty and improve accuracy. Ensuring that data continue to be open and free to the public is also important from a transparency perspective. Vulnerability data and analyses are important areas for climate and energy researchers to focus their efforts on. As our pilot has shown, different generation and cooling technologies can have very different levels of vulnerability to climate change. The continued efforts by international organizations and regulatory agencies to recommend or mandating companies to disclose more on climate risks and vulnerabilities present an opportunity for climate science and risk assessment to achieve better robustness and comprehensiveness.

Methods
Here we present a brief description of the methodology. For more details on methodology and data and threshold sources, please refer to the Methodology section in the Supplementary Information document.

Droughts-induced thermal power-generation losses. We assessed drought risk for thermal power plants using the 12-month Standardized Precipitation-Evapotranspiration Index (SPEI) following a previous study[31]. (Supplementary Fig. 4). SPEI was used as a proxy of water availability in this study. We converted monthly SPEI into estimated disruption hours using the vulnerability factors table (Supplementary Table 1) following Eq. (1).

$$DH_{annual}(x) = \frac{\sum_{1}^{n} VF(x)}{n} * c * (365 * 24)$$ (1)

where DH_{annual} is the total number of disruption hours in a calendar year, $VF(x)$ is the interpolated vulnerability factor for a given x, n is the number of records in a time series, c is a constant converting the time step into a daily time step.

With the installed capacity of each unit, annual estimated generation losses (EGL) caused by drought were calculated following Eq. (2).

$$GL_{annual} = P * DH_{annual}$$ (2)

where GL_{annual} is the estimated annual generation losses in MWh, DH_{annual} is the total number of disruption hours in a calendar year, P is the installed capacity in MW.

Floods-induced thermal plant generation losses. We assessed direct flood risks with a probabilistic approach derived following ref. [32], using globally modeled riverine and coastal inundation datasets[33,34] (Supplementary Fig. 5). For each plant, period-RCP-GCM-specific loss-probability curves were derived from the depth-probability curves by converting inundation depth to corresponding vulnerability factors (Supplementary Table 1). The annual total disruption days for both the baseline and future period were calculated following Eq. (3). A default 250-year flood protection standard[35] was applied to all plants (except for nuclear plants which are protected against 10,000-year floods) in the calculation, meaning floods smaller than a 250-year (10,000-year for nuclear plants) event would have

no impact on the unit/plant.

$$DH_{annual} = \int_{0}^{P} LP(p_i) * 24$$ (3)

where DH_{annual} is the total number of disruption hours in a calendar year, p refers to probability or corresponding return period, P is the designed flood protection level or corresponding return period, $LP(p_i)$ is the loss-probability function derived from the depth-probability curve combined with vulnerability factors (Supplementary Table 1).

With the installed capacity of each unit, annual EGL caused by floods for both the baseline and future periods were calculated following Eq. (2).

Air temperature-induced thermal plant generation losses. We assessed air temperature risks using an approach derived based on the principle of the analytical framework developed by Ward et al. [33] (Supplementary Fig. 6). Two plant-specific thresholds, i.e., desired air temperature (DAT) and shut down air temperature (SAT), and pre-defined vulnerability factors (Supplementary Table 1) following air temperature-efficiency relationships established by Şen et al. [36] were used to quantify air temperature rise-induced power-generation losses. Days with air temperature above SAT and below DAT were assigned 24 h and 0 h of disruption, respectively. When air temperatures fall in between DAT and SAT, their differences from DAT were calculated and used to look up corresponding vulnerability factors from Supplementary Table 1. The interpolated vulnerability factors were then converted into annual total disruption hours following Eq. (1). With the installed capacity of each unit, the annual EGL caused by air temperature rise was calculated following Eq. (2).

Water temperature-induced thermal plant generation losses. We assessed water temperature risks based on pre-defined relationships between generation efficiency reduction and cooling water temperature and/or wet-bulb temperature (Supplementary Fig. 7). We assigned 32 °C[24] as the default intake water temperature limit, which corresponds to ~42 °C discharge water temperature according to the linear relationship between intake and discharge water (Eq. 4). For areas subject to discharge water regulations, when water temperature exceeds the limit, once-through cooling plants are expected to be curtailed partially or completely. For cases where the water temperature were lower than regulatory limits, they were compared to desired water temperature (DWT). Differences in degrees Celsius from DWT were calculated and used to look up corresponding vulnerability factors (Supplementary Table 1). The interpolated vulnerability factors were then converted into annual total disruption hours following Eq. (1).

$$t_o = 1.0191 * t_i + 9.7951$$ (4)

where t_o is the outlet (discharge) water temperature, t_i is the intake water temperature.

With the installed capacity of each unit, the annual EGL caused by air temperature rise was calculated following Eq. (2).

Recirculating steam turbines become vulnerable to water temperature rise when the WBT exceeds its design temperature, the 99th percentile (p99) of the local, historical time series[24]. We calculated outlet water temperature as a function of water temperature (Eq. (4)). If outlet water temperature exceeds the design temperature, the degree differences were calculated and used to look up vulnerability factors from Supplementary Table 1. The interpolated vulnerability factors were then converted into annual total disruption hours following Eq. (1).

With the installed capacity of each unit, the annual EGL caused by air temperature rise was calculated following Eq. (2).

Water stress-induced thermal plant generation losses. The water stress metric in this assessment primarily accounts for reduced water availability caused by increased upstream consumptive water uses (Supplementary Fig. 8), which is different from the drought metric (i.e., SPEI) as it merely reflects meteorological conditions. The water stress ratio (WS) in a given catchment was calculated following Eq. (5). Generation losses are calculated when WS is high or extremely high (or greater than 40%[37]).

$$WS = \frac{WW}{BA}$$ (5)

where WW is the total water withdrawal, BA is the total available blue water supply.

In areas with high or extremely high water stress, it is often likely that more stringent water efficiency targets[38] and water use limits[39,40] would gradually take place to cope with chronic issues or be introduced suddenly to address unexpected disruptions caused by acute events. It is probable that a reduced water availability, regardless of its driver (less supply or more demand), will lead to higher standards on water use limit and a lower water budget for users. The supply reduction rate (SRR, i.e., percent change of the future blue water availability from baseline) was calculated following Eq. (6). The vulnerability factors which indicate the percent capacity that is stranded due to a limited cooling water budget were then interpolated from Supplementary Table 1. The interpolated vulnerability factors

were then converted into annual total disruption hours following Eq. (1).

$$SRR = \frac{BW_{proj} - BW_{ba}}{BW_{ba}} \qquad (6)$$

where BW_{proj} is the projected blue water availability, BW_{ba} is the historical blue water availability.

With the installed capacity of each unit, the annual EGL caused by water temperature rise was calculated following Eq. (2).

Ensemble analysis. We used an ensemble approach by aggregating GCM-specific annual generation losses for each unit and each module. In brief, in each run, six statistics, i.e., median, p10, p90, mean, minimum, and maximum, were reported for historical annual generation losses and the future projections under RCP4.5 and RCP8.5 for each unit. Medians demonstrate the result derived from a typical GCM. The p10 and p90 values indicate GCM-induced uncertainties. The unit-level statistics were added up to account for the plant-level impacts. To quantify portfolio-level impacts, we further grouped plant-level generation losses by risk types.

Sensitivity analysis. We conducted a sensitivity analysis to assess how generation losses vary with different design thresholds of water temperature, air temperature, and flood protection level. For the design thresholds of water temperature and air temperature, we selected four commonly used percentiles in physical climate risk assessment (i.e., p75, p90, p95, p99). Table 4 shows that the generation losses related to water and air temperature will increase in the future under all design thresholds, whereas flood-related generation losses will decrease. The summary statistics excludes plants that are not impacted by specific hazard, which is why the plant count of three hazards appear to be different in Table 4. For water temperature, air temperature, and flood protection level, the generation losses in baseline and projection periods are negatively related to the design threshold levels.

Validation for thermal power-generation losses. Given that Uran and Valuthur are CCGT plants which are often used for providing additional supply when electricity demand is high during peak hours, we suspect the clusters represent two distinct operating schemes intentionally planned and managed by local utility companies, serving different schedules. We then applied clustering analyses using DBSCAN with multiple hypotheses, e.g., 2, 3, and 4 clusters, and found that a two-cluster segregation makes the most sense compared to others. Generation data points outside the two clusters could be electricity generated on days when there was an unusually high demand or RSD (Reserved Shutdowns) planned by local grids.

In the plant-level validation, high air temperature-induced generation losses are calculated as the difference between maximum power generation under the ideal operation condition (i.e., the 90th percentile of all air temperature observations) and the modeled power generation as a function of air temperature relative to the designed maximum power generation (Eq. (7)). Plant-level generation loss was taken as the sum of generation loss for each cluster.

$$GL(T \geq T_{90}) = \frac{\sum_{T_{90}}^{T_{max}}((aT_{90} + b) - (aT + b))}{Cap * N * 24} \qquad (7)$$

Where GL stands for generation losses in GWh, T refers to air temperature in degree Celsius, T_{90} refers to the 90th percentile of air temperatures over the study period, T_{max} refers to the maximum air temperature over the study period, a and b refer to the slope and intercept of the linear relationship between power generation in MWh and air temperature in degrees Celsius, Cap refers to installed capacity in MW, N refers to the number of days in records.

Hydroelectric power plant assessment. We first identified the watershed (including all upstream areas) that the hydro plant is located in based on its geolocation. We then calculated the mean air temperature and sum of total precipitation and water consumption within the watershed boundaries for each month over three different timeframes with corresponding datasets (and models when applicable). We used ERA5 climate reanalysis for the historical period (1980–2014), and NEX-GDDP climate projections for the backcast period (1980–2005) and projection period (2010–2049). A quantile-mapping-based bias-correction was conducted on the NEX-GDDP future projections against the ERA5 reanalysis. Water consumption data came from the Aqueduct 3.0 Behind-the-Scenes dataset.

For the hydro plants of which historical generation data were not available, we estimate plants' potential generation changes in the future based on their upstream precipitation and water consumption changes between now and 2030. We do not attempt to model any dam structure damage-related disruptions that may or may not be caused by climate hazards, as that requires detailed dam-specific design information and is not a viable approach for this type of exercise. For hydro plants which we have historical monthly generation data, we explore and apply a machine-learning regression model that estimates generation using precipitation, air temperature, upstream water use, and operation disruption data.

A variety of regression models including support vector regression models, fixed effect models, and machine-learning regression models such as LSTM, were tested in this study. A LSTM regression model was chosen based on its higher

Table 4 Sensitivity analysis of generation losses (MWh) related to water temperature, air temperature, and floods under different design thresholds.

Design threshold	Plant count	Baseline					2030 RCP4.5					2030 RCP8.5				
		median	min.	p5	p95	max.	median	min.	p5	p95	max.	median	min.	p5	p95	max.
Water temperature																
p75	19	38,194	1086	3751	1,116,031	1,300,254	383,721	10,403	16,270	4,161,051	7,564,012	451,892	17,385	18,784	4,712,556	9,318,046
p90	19	29,256	210	586	975,420	1,064,925	253,909	4110	5150	3,918,440	7,512,261	274,893	5023	10,007	4,479,417	9,263,436
p95	19	29,256	77	473	820,903	1,035,207	250,091	1773	4876	3,923,384	7,399,219	274,893	2624	9696	4,471,987	9,159,505
p99	19	29,256	77	473	320,041	511,068	249,120	1773	4876	3,369,379	6,646,063	274,893	2624	7609	3,984,028	8,311,164
Air temperature																
p75	7	137,030	15,770	26,072	254,902	256,172	306,376	33,609	48,501	571,476	628,301	333,862	36,457	52,453	635,264	703,416
p90	7	29,018	4176	6,605	63,245	67,052	132,511	14,688	19,344	258,930	301,724	132,882	16,619	21,537	308,877	360,886
p95	7	11,968	1854	2,788	27,219	29,734	81,282	8640	10,736	163,143	194,115	77,532	10,250	12,570	206,088	245,338
p99	7	1960	348	466	4621	5167	30,765	2507	3024	63,779	74,875	27,367	3538	4099	89,461	106,906
Flood protection level																
1/100	5	82,130	325	913	363,147	429,197	33,614	131	256	466,060	521,673	42,442	596	963	324,200	365,941
1/250	5	31,701	149	720	130,154	149,481	11,661	138	201	159,509	170,356	15,151	339	705	97,242	99,235
1/500	5	10,932	63	495	45,019	49,827	3871	91	122	96,841	114,224	4,834	175	449	52,944	59,910

performance in estimating generation compared to other methods tested. Previous hydrology-focused studies[41] have also argued for higher effectiveness of LSTM models over that of traditional statistical methods.

There are three features used in our model including, adjusted precipitation, air temperature, and disruption. Adjusted precipitation is calculated as the total precipitation in the watershed minus total water consumption. Disruption is historical plant shut down records or operations log data shared by EBRD. The target data of our model is the power plant's historical actual monthly generations shared by EBRD.

As shown in Supplementary Fig. 9, we created our base model using the Keras–Tensorflow LSTM module with 100 neurons, 300 epochs, a dropout rate of 0.1, and a recurrent dropout rate of 0.2. Four model parameters were made adjustable, including look-back, batch size, optimizer, and loss function. For model tuning, we tested 180 combinations of those four parameters, and ran the training process 50 times independently for each combination. We diagnosed if the model was under or over-fitting by running the same combination 400 times and evaluating the epoch-loss curves of training and testing sets. Only models with two converging trends (indicating good fit) epoch-loss curves are selected as valid candidates. We then selected the one trained model with the best performance (e.g., highest r-squared value) as the final generation estimation model for the power plant.

Once the plant-specific model is selected, we then feed it with the model- and scenario-specific GDDP projections, and projected future monthly generation for the future period.

For developing the machine-learning model, the actual historical generation time series dataset is split into a training set (the first 70% of data of the time series) and a testing one (the remaining 30%). Data from the testing set were never seen by the models during their training processes. We achieve unseen testing set validation with a R-squared value at about 0.62, as shown in Supplementary Fig. 10.

Key limitations. Current climate science, available global datasets, and unit-specific information on assets all have their limitations, and there is room to improve our modeling approach.

Solar and wind projects were excluded from this study, as several earlier project-level assessments commissioned by EBRD suggested that those technologies are less sensitive to physical climate hazards than thermal and hydro generation. Thermal and hydro generation represents ~58% of EBRD's financial exposure amongst power-generation technologies.

The Aqueduct global flood inundation maps used for assessing flood risks have a one square kilometer spatial resolution, and cover only large-scale riverine flood and coastal storm surge with sea-level rise taken into account. The spatial resolution is relatively coarse for risk assessment at the facility level. Flash and groundwater floods are not included, because no such data are available at the global scale in the public domain.

Some global climate and hydrology datasets adopted in our assessment use different forcing data. For example, the water temperature data from ref. [42] is forced with ERA-40 and ERA-Interim, but air and dew point temperatures used for calculating wet-bulb temperatures are from ERA5, which introduces potential comparability limitations to our assessment process. However, quantile-mapping-based bias corrections are conducted, aiming to minimize limitations in comparing indicators with different forcing data.

We use the 12-month Standardized Precipitation-Evapotranspiration Index (SPEI) drought index to model water levels in rivers and/or reservoirs; however, it may not accurately reflect water availability in these water bodies. Twelve-month SPEI drought index uses meteorological data, including precipitation, temperature, and evapotranspiration to approximate changes in streamflow, a hydrological variable. The correlation between SPEI and streamflow is generally very high, but can vary in different river basins[43]. In addition, we calculate 12-month SPEI using outputs from seven CMIP5 climate models. The grid resolution of these models can be as large as 2.0225° by 2.5°, or about 224 km by 278 km at the equator[44]. We may not simulate precise local conditions using coarse resolutions.

Indirect impacts, e.g., grid and fuel storage and transportation exposure to wildfire, cold snaps, and floods, and disruptions to fuel transportation and staff commuting due to floods and other factors are not accounted for. The indirect impact can be severe and sometimes detrimental to power-generating assets[45]. Impact on electricity demand was not studied either. Due to limitations on the necessary data needed for conducting indirect impact assessment at a global scale, we decided to focus on assessing direct impact.

Spatial and temporal correlations between hazards as well as grid effects on power-generation volatility are not explicitly included in our modeling efforts. Climate-related physical hazards are correlated both spatially and temporally. Power plants in a large geographical area could be exposed to multiple hazards and lose generation capacity simultaneously. We analyze impacts from these hazards individually but these impacts could aggregate and result in larger generation loss. There is also a systemic risk if all power plants in a large area lose power, a scenario we do not analyze in this paper.

Although we collect and use hazard- and technology-specific vulnerability factors to determine how hazards affect power plant generation, the vulnerability of one power plant could be different from another power plant even if they are using the same technology. For example, we use the same water temperature threshold for thermal power plants using wet-cooled power plants, but these power plants could be designed or optimized to operate at different tower dimensions, water consumption rates, exit air temperature, etc.[46,47]. The design and optimization differences could result in varying vulnerabilities to hazards.

2030 is selected as the assessment horizon for our study based on consultations with EBRD, as ten years into the future is the most relevant timeframe for the bank in terms of internal strategy-making and external communications with its clients for practical reasons. However, there are benefits of extending the horizon beyond 2030. For example, portfolio-level physical climate risks could really increase exponentially in decades after 2030 under high emission scenarios, as effects of climate change scenarios on hazard severity start to kick in around 2030. The climate and water projection data we used in our method allow for extending horizons to 2100.

Data availability

All data used in this manuscript are made available. Plant-specific climate and hazard time series (i.e., air temperature, wet-bulb temperature, precipitation, drought, floods, and water temperature) that support the findings of this study are available in ref. [48], which are also the source data for Fig. 3. Source data for Fig. 4 are in Table 2 in the main text. Source data for Figs. 5 and 6 and Supplementary Figs. 2 and 3 can be found in Supplementary Data 1[49]. Unit-level daily outage data for thermal power plants in India from April 1, 2013 through March 31, 2017 which was used for validation can be found in Supplementary Data 2[50]. Vulnerability factors are available in Supplementary Table 1. An anonymized version of the power plants in EBRD's early 2021 portfolio can be found in Supplementary Data 3[51]. The actual generation data used in the machine-learning-based hydropower plant assessment as shown in Supplementary Fig 10 can be found in Supplementary Data 4[52].

Code availability

Scripts that support the assessment are available from the corresponding author upon reasonable request for non-commercial purposes.

References

1. Gambhir, A. et al. Near-term transition and longer-term physical climate risks of greenhouse gas emissions pathways. *Nat. Clim. Chang.* **12**, 88–96 (2022).
2. Fiedler, T. et al. Business risk and the emergence of climate analytics. *Nat. Clim. Chang.* **11**, 87–94 (2021).
3. Hultman, N. E., Hassenzahl, D. M. & Rayner, S. Climate risk. *Annu. Rev. Environ. Resour.* **35**, 283–303 (2010).
4. Bingler, J. A. & Colesanti Senni, C. Taming the Green Swan: a criteria-based analysis to improve the understanding of climate-related financial risk assessment tools. *Clim. Policy* **22**, 356–370 (2022).
5. Ebinger, J. O. & Vergara, W. Climate impacts on energy systems: key issues for energy sector adaptation. https://openknowledge.worldbank.org/handle/10986/2271 (2011).
6. Yalew, S. G. et al. Impacts of climate change on energy systems in global and regional scenarios. *Nat. Energy* **5**, 794–802 (2020).
7. Schaeffer, R. et al. Energy sector vulnerability to climate change: a review. *Energy* **38**, 1–12 (2012).
8. Cronin, J., Anandarajah, G. & Dessens, O. Climate change impacts on the energy system: a review of trends and gaps. *Clim. Change* **151**, 79–93 (2018).
9. van Vliet, M. T. H. et al. Vulnerability of US and European electricity supply to climate change. *Nat. Clim. Change* **2**, 676–681 (2012).
10. Khan, I., Alam, F. & Alam, Q. The global climate change and its effect on power generation in Bangladesh. *Energy Policy* **61**, 1460–1470 (2013).
11. Zhou, Y., Panteli, M., Wang, B. & Mancarella, P. Quantifying the system-level resilience of thermal power generation to extreme temperatures and water scarcity. *IEEE Syst. J.* **14**, 749–759 (2020).
12. Lohrmann, A., Farfan, J., Caldera, U., Lohrmann, C. & Breyer, C. Global scenarios for significant water use reduction in thermal power plants based on cooling water demand estimation using satellite imagery. *Nat. Energy* **4**, 1040–1048 (2019).
13. Liao, X., Hall, J. W. & Eyre, N. Water use in China's thermoelectric power sector. *Global Environ. Change* **41**, 142–152 (2016).
14. Liu, L., Hejazi, M., Li, H., Forman, B. & Zhang, X. Vulnerability of US thermoelectric power generation to climate change when incorporating state-level environmental regulations. *Nat. Energy* **2**, 1–5 (2017).
15. Bennett, J. A. et al. Extending energy system modelling to include extreme weather risks and application to hurricane events in Puerto Rico. *Nat. Energy* **6**, 240–249 (2021).

16. Gruber, K., Gauster, T., Laaha, G., Regner, P. & Schmidt, J. Profitability and investment risk of Texan power system winterization. *Nat. Energy* **7**, 409–416 (2022).

17. Ahmad, A. Increase in frequency of nuclear power outages due to changing climate. *Nat. Energy*. https://doi.org/10.1038/s41560-021-00849-y (2021).

18. Perera, A. T. D., Nik, V. M., Chen, D., Scartezzini, J.-L. & Hong, T. Quantifying the impacts of climate change and extreme climate events on energy systems. *Nat. Energy* **5**, 150–159 (2020).

19. IPCC. *Climate Change 2014: Impacts, Adaptation, and Vulnerability: Working Group II Contribution to the Fifth Assessment Report of the Intergovernmental Panel on Climate Change* (Cambridge University Press, 2014).

20. Global Energy Observatory, Google, KTH Royal Institute of Technology in Stockholm, Enipedia, World Resources Institute. Global Power Plant Database. Published on Resource Watch and Google Earth Engine; http://resourcewatch.org/ https://earthengine.google.com/ (2018).

21. EU Technical Expert Group on Sustainable Finance. *Financing a Sustainable European Economy. Taxonomy Report: Technical Annex.* https://ec.europa.eu/info/sites/info/files/business_economy_euro/banking_and_finance/documents/200309-sustainable-finance-teg-final-report-taxonomy-annexes_en.pdf (2020).

22. Pinchot, A., Zhou, L., Christianson, G., McClamrock, J. & Sato, I. Assessing physical risks from climate change: do companies and financial organizations have sufficient guidance? *WRIPUB.* https://doi.org/10.46830/wriwp.19.00125 (2021).

23. van Vliet, M. T. H., Wiberg, D., Leduc, S. & Riahi, K. Power-generation system vulnerability and adaptation to changes in climate and water resources. *Nat. Clim. Change* **6**, 375–380 (2016).

24. Hamanaka B., Zhao H., & Sharpe P. Comparison of advanced cooling technologies efficiency depending on outside temperature. INL/EXT-09-17392, 969508. http://www.osti.gov/servlets/purl/969508-yh9nVb/ (2009).

25. Macknick, J. et al. Water and climate impacts on power system operations: the importance of cooling systems and demand response measures. NREL/TP--6A20-66714, 1338177. http://www.osti.gov/servlets/purl/1338177/ (2016).

26. Liu, L., Hejazi, M., Li, H., Forman, B. & Zhang, X. Vulnerability of US thermoelectric power generation to climate change when incorporating state-level environmental regulations. *Nat. Energy* **2**, 17109 (2017).

27. Luo, T., Krishnan, D. & Sen, S. *Parched Power: Water Demands, Risks, and Opportunities for India's Power Sector* (Water Resource Institute, 2018).

28. CEA. Annual report 2017-18. https://cea.nic.in/old/reports/annual/annualreports/annual_report-2018.pdf (2018).

29. Hersbach, H. et al. The ERA5 global reanalysis. *Q.J.R. Meteorol. Soc.* **146**, 1999–2049 (2020).

30. Ester, M., Kriegel, H.-P., Sander, J. & Xu, X. A density-based algorithm for discovering clusters in large spatial databases with noise. In *Proceedings of the 2nd International Conference on Knowledge Discovery and Data Mining.* Vol. 96 226–231 (Institute for Computer Science, 1996).

31. Zhou, L., Mcclamrock, J., Christianson, G., Krishnan, D. & Luo, T. Financial implications of parched power: insights from an analysis of Indian thermal power companies. **56**. https://files.wri.org/s3fs-public/financial-implications-parched-power_2.pdf (2019).

32. Ward, P. J. et al. Assessing flood risk at the global scale: model setup, results, and sensitivity. *Environ. Res. Lett.* **8**, 044019 (2013).

33. Ward, P. J. et al. AQUEDUCT FLOODS METHODOLOGY. **28**. https://www.wri.org/publication/aqueduct-floods-methodology (2020).

34. Winsemius, H. C., Van Beek, L. P. H., Jongman, B., Ward, P. J. & Bouwman, A. A framework for global river flood risk assessments. *Hydrol. Earth Syst. Sci.* **17**, 1871–1892 (2013).

35. Schulz, J. GIS-based flood risk management for thermal power plants in Germany. In *The Economic, Social and Political Elements of Climate Change* (ed. Leal Filho, W.) 301–309 (Springer, 2011).

36. Şen, G. et al. The effect of ambient temperature on electric power generation in natural gas combined cycle power plant—a case study. *Energy Rep.* **4**, 682–690 (2018).

37. Vorosmarty, C. J. Global water resources: vulnerability from climate change and population growth. *Science* **289**, 284–288 (2000).

38. CEA. *National Electricity Plan (Volume I) Generation* (CEA, 2018).

39. Rogers, P. Drought or no drought: Jerry Brown sets permanent water conservation rules for Californians. *The Mercury News.* https://www.mercurynews.com/2018/05/31/california-drought-jerry-brown-sets-permanent-water-conservation-rules-with-new-laws/ (2018).

40. Mahr, K. How Cape Town was saved from running out of water. *The Guardian.* https://www.theguardian.com/world/2018/may/04/back-from-the-brink-how-cape-town-cracked-its-water-crisis (2018).

41. Kratzert, F., Klotz, D., Brenner, C., Schulz, K. & Herrnegger, M. Rainfall–runoff modelling using long short-term memory (LSTM) networks. *Hydrol. Earth Syst. Sci.* **22**, 6005–6022 (2018).

42. Wanders, N., Vliet, M. T. H., Wada, Y., Bierkens, M. F. P. & Beek, L. P. H. (Rens) High-resolution global water temperature modeling. *Water Resour. Res.* **55**, 2760–2778 (2019).

43. Vicente-Serrano, S. M. & Beguería, S. Comment on "Candidate Distributions for Climatological Drought Indices (SPI and SPEI)" by James H. Stagge et al. *Int. J. Climatology* **36**, 2120–2131 (2016).

44. ENES. CMIP5 models and grid resolution. https://portal.enes.org/data/enes-model-data/cmip5/resolution (2019).

45. PG&E. PG&E achieves bankruptcy court confirmation of its plan of reorganization. https://www.pge.com/en/about/newsroom/newsdetails/index.page?title=20200620_pge_achieves_bankruptcy_court_confirmation_of_its_plan_of_reorganization (2020).

46. Leeper, S. A. Wet cooling towers: rule-of-thumb design and simulation. https://www.osti.gov/biblio/5281927 (1981).

47. Dincer, I., Rosen, M. A. & Ahmadi, P. Modeling and optimization of power plants. In *Optimization of Energy Systems* (ed. Cheng, Y.) 275–316 (John Wiley & Sons, Ltd, 2017).

48. Cheng, Y. & Luo, T. Plant-specific climate and hazard time series. *Figshare.* https://figshare.com/articles/dataset/_/22241743 (2023).

49. Cheng, Y. & Luo, T. Supplementary Data 1—figure data.xlsx. *Figshare.* https://figshare.com/articles/dataset/_/22241074 (2023).

50. Luo, T. & Cheng, Y. Supplementary Data 2—unit-level daily outage data for thermal power plants in India used for validation. *Figshare.* https://figshare.com/articles/dataset/_/22241089 (2023).

51. Luo, T. & Cheng, Y. Supplementary Data 3—anonymized version of the power plants in EBRD's early 2021 portfolio. *Figshare.* https://figshare.com/articles/dataset/_/22262815 (2023).

52. Luo, T. & Cheng, Y. Supplementary Data 4—actual generation data used in the machine learning-based hydropower plant assessment. *Figshare.* https://figshare.com/articles/dataset/_/22262854 (2023).

53. Barbarossa, V. et al. Threats of global warming to the world's freshwater fishes. *Nat. Commun.* **12**, 1701 (2021).

54. Taylor, K. E., Stouffer, R. J. & Meehl, G. A. An overview of CMIP5 and the experiment design. *Bull. Am. Meteorol. Soc.* **93**, 485–498 (2012).

55. Gassert, F., Luck, M., Landis, M., Reig, P. & Shiao, T. Aqueduct Global Maps 2.1: Constructing Decision-Relevant Global Water Risk Indicators. Working Paper. (World Resources Institute, Washington, DC, 2014). Available online at http://www.wri.org/publication/aqueduct-globalmaps-21-indicators.

56. Luck, M., Landis, M. & Gassert, F. Aqueduct Water Stress Projections: Decadal Projections of Water Supply and Demand Using CMIP5 GCMs. Technical Note. (World Resources Institute, Washington, D.C., 2015). Available online at: https://www.wri.org/publication/aqueduct-water-stress-projections.

57. Vicente-Serrano, S. M., Beguería, S. & López-Moreno, J. I. A multiscalar drought index sensitive to global warming: the standardized precipitation evapotranspiration index. *J. Clim.* **23**, 1696–1718 (2010).

Author contributions

T.L. conceived the original idea, reviewed literature, developed the model, curated data, developed the code, and wrote the manuscript. Y.C. developed the model, developed the code, and wrote the manuscript. J.F. conceived the original idea and wrote the manuscript. J.K. reviewed literature and wrote the manuscript. L.Z. conceived the original idea, reviewed literature, curated data, and wrote the manuscript. Y.W. wrote the manuscript. A.H. wrote the manuscript.

Competing interests

The authors declare no competing interests.

Additional information

Supplementary information The online version contains supplementary material available at https://doi.org/10.1038/s43247-023-00782-w.

Correspondence and requests for materials should be addressed to Tianyi Luo.

Peer review information *Communications Earth & Environment* thanks the anonymous reviewers for their contribution to the peer review of this work. Primary Handling Editors: Heike Langenberg. Peer reviewer reports are available.

Reprints and permission information is available at http://www.nature.com/reprints

Publisher's note Springer Nature remains neutral with regard to jurisdictional claims in published maps and institutional affiliations.